JCTC Journal of Chemical Theory and Computation

Effect of Water Polarizability on the Properties of Solutions of Polyvalent Ions: Simulations of Aqueous Sodium Sulfate with Different Force Fields

Erik Wernersson* and Pavel Jungwirth

Institute of Organic Chemistry and Biochemistry, Academy of Sciences of the Czech Republic, and Center for Biomolecules and Complex Molecular Systems, Flemingovo nám. 2, 16610 Prague 6, Czech Republic

Received August 18, 2010

Abstract: We show that aqueous sodium sulfate solutions exhibit an unrealistically large degree of ion pairing and clustering when modeled using nonpolarizable force fields, with clusters resembling precipitate readily forming in a 0.5 m solution at ambient conditions. This aggregation behavior was found to be persistent in nonpolarizable water for a range of parameters of the sulfate anion. In contrast, a polarizable potential performs satisfactorily, producing a well dissolved salt with a degree of association that is consistent with activity data for real solutions. Most of this improvement is due to polarization of water molecules in the vicinity of the divalent sulfate anion, which enhances its solvation.

1. Introduction

For computer simulations to be a useful aid for understanding the role of ions in complex chemical and biological systems, it is essential that realistic force fields are used. A necessary condition for an ionic force field to be considered realistic is that it gives a correct account of the properties of simple salt solutions. We have observed that a commonly used set of sulfate parameters[1] together with the Smith−Dang sodium parameters[2] in SPC/E water lead to formation of clusters, reminiscent of crystallites, of sodium sulfate well below the experimental solubility limit of 2 m at 25 °C.[3] Similar aggregation has been reported from molecular dynamics (MD) simulations of ammonium sulfate in SPC/E, TIP3P Ewald, and TIP3P-F water[4] with a different set of sulfate parameters.[5] This suggests that the problem of spurious clustering is not unique to a particular sulfate parametrization or salt. A polarizable version[6] of the sulfate model of ref 1, neutralized by Smith−Dang sodium ions[2] in polarizable POL3 water, has been applied to the study of the interfacial behavior of sulfate.[7] In that work, excessive cluster formation was not observed.

The fact that similar ionic force fields predict dramatically different aggregation behavior in nonpolarizable vs polarizable simulations suggests that polarizability may be important for proper description of interactions between sodium and sulfate ions in water. To investigate this issue in detail, we made a systematic comparison of different variants of the sulfate model proposed in ref 1 in combination with different sodium and water models. In order to enable comparison with experiments, we analyzed the simulations in terms of the Kirkwood−Buff (KB) theory.[8] Within this theoretical framework, the integrals of the radial distribution functions, which are readily obtainable from simulations, can be related to the concentration derivatives of thermodynamic quantities such as chemical potentials and partial molar volumes. The deviation of the salt chemical potential from ideality gives a measure of the overall degree of association in the solution. Comparison with this quantity is, therefore, a suitable way to ascertain whether the association behavior seen for a given set of parameters is realistic.

2. Simulation Details

We performed MD simulations of sodium sulfate in aqueous solution. The simulation box contained 12 sulfate and 24 sodium ions together with 1395 water molecules, which yielded a solution with a concentration of 0.48 m. After 0.5 ns equilibration, the trajectories were propagated in 10 ns increments until the radial distribution functions were well

* To whom correspondence should be addressed: E-mail: erik.wernersson@uochb.cas.cz.

10.1021/ct100465g
Published on Web 09/23/2010

Table 1. Force Field Parameters

model	atom	σ (Å)	ε (kcal/mol)	q
sulfate 1	S	3.55	0.250	2.4
	O	3.15	0.250	−1.1
sulfate 2[a]	S	3.55	0.250	2.0
	O	3.15	0.200	−1.0
sulfate 3	S	3.55	0.250	2.8
	O	3.15	0.200	−1.2
sulfate 4	S	3.55	0.250	1.6
	O	3.15	0.200	−0.9
sulfate 5	S	3.55	0.250	2.0
	O	3.213	0.200	−1.0
sulfate 6	S	3.55	0.250	2.0
	O	3.087	0.200	−1.0
sodium 1[b]	Na	2.35	0.130	1.0
sodium 2	Na	2.73	0.100	1.0

[a] Used in the polarizable simulations with an oxygen polarizability of 1.0 Å^3 and a sulfur polarizability of zero. [b] Used in the polarizable simulations with a polarizability of 0.24 Å^3.

Table 2. Summary of the Different Combinations of Sulfate, Sodium, and Water Models Considered

run	water	sulfate model	sodium model	time (ns)	clusters[a]
1	SPC/E	1	1	20	y
2	SPC/E	2	1	30	y
3	SPC/E	3	1	20	y
4	SPC/E	4	1	10	y
5	SPC/E	5	1	10	y
6	SPC/E	6	1	20	y
7	SPC/E	2	2	30	n
8	TIP4P/2005	2	1	20	n
9	SPC/E	2[b]	1[b]	10	y
10	POL3	2[c]	1[c]	20	n
11	POL3	2	1	20	n
12	Dang-Chang	2	1	30	n

[a] Refers to persistent clusters; some degree transient clustering was seen in all solutions. [b] Polarizable ions. [c] Nonpolarizable ions.

converged or until persistent clusters had formed. The cutoff for short-range interactions was set to 12.0 Å. Long-range electrostatic interactions were accounted for with the use of the particle mesh Ewald method.[9] In all polarizable simulations, the induced dipoles of all atoms were self-consistently converged at each time step. The temperature in all simulations was kept at 300 K using the Berendsen weak coupling algorithm, and the pressure was held constant at 1 atm using an analogous algorithm.[10] The AMBER 10 molecular dynamics package was used for all calculations.[11]

In this study, we focused on the effects of the details of the force field parametrization on the properties of sodium sulfate solutions. In ref 1, two alternative sets of sulfate parameters were suggested. Sulfate model 1 (using the same numbering as in ref 1) has charges of −1.1 e placed on each oxygen whereas sulfate model 2 has on each oxygen a partial charge of −1.0 e. As sulfate model 2 is the one that forms the basis for the polarizable model from ref 6, it is adopted here as the reference sulfate model. To investigate the influence of the sulfate partial charges with fixed Lennard−Jones parameters, we additionally considered two variants of sulfate model 2, denoted as sulfate models 3 and 4, with oxygen partial charges of −0.9 and −1.2 e, respectively. Also, variations in the Lennard−Jones σ parameter of oxygen were considered. Sulfate models 5 and 6 have σ reduced and increased, respectively, by 2% compared to sulfate model 2. The Lennard−Jones parameters and partial charges for all sulfate models considered are summarized in Table 1. To assess the importance of the cation parameters, we have used two different models of the sodium cation. Sodium model 1 is the one by Smith and Dang,[2] while sodium model 2 is taken from ref 12; see Table 1.

Next, we included polarizability into the force field. In ref 6, the polarizability of sulfate was determined, on the basis of ab initio MD simulations, to be almost isotropic with a value of about 7.1 Å^3. Because most of the electron density from the frontier orbitals was located on the oxygens, the authors suggested that the total polarizability should be evenly divided between the four oxygen atoms. The resulting model with a polarizability of 1.775 Å^3 on each oxygen atom could not be used directly as the iterative procedure used to calculate the induced dipole moment diverged due to the so-called polarization catastrophe.[13] Therefore, we used a reduced value of 1.0 Å^3 for the polarizability of each of the oxygens in all sulfate models. For sodium, the polarizability of 0.24 Å^3 was used.[2]

Four water models were considered, two polarizable and two nonpolarizable (see Table 2). The polarizable ones were the POL3[14] and Dang−Chang[15] models and the nonpolarizable ones were SPC/E[16] and TIP4P/2005.[17] Polarizable water models were combined with polarizable ions and vice versa, unless otherwise stated. The POL3 and SPC/E models were chosen since they have been previously used with the polarizable and nonpolarizable sulfate models, respectively. The two other models, which are more recent and refined, were chosen for comparison. In the POL3 model, the polarizability is partitioned between the oxygen and hydrogen atoms. In the Dang−Chang model, the only polarizable site is the auxiliary site on the H−O−H bisector.[14,15] The models thus differ, among other things, in the details of how the polarizability is handled. Comparison between these two models is, therefore, useful for discerning whether the polarizability itself, as opposed to other differences between them, is important for the qualitative behavior of the system. In order to assess separately the influence of the polarizability of the ions and water, we also performed simulations of polarizable ions in SPC/E water and of nonpolarizable ions in POL3 water.

Additionally, in order to analyze in detail polarization of water in the hydration shell of sulfate, we simulated a small system with one sulfate ion (model 2) and 512 water molecules for each of the polarizable water models above. For technical reasons related to the calculation of the induced dipole moment in AMBER 10, these simulations were done at constant volume. The volume was determined as the average volume from a 0.5 ns test run at constant pressure. The system was equilibrated for 0.5 ns, and data were collected during the following 1 ns. Similar calculations in POL3 water were carried out for sodium (model 1) as well as for a test monovalent variant of sulfate model 2 where all partial charges were halved.

Table 3. Values of Γ Calculated from Experimental Activity Coefficients

m (mol/kg)	Γ
0.15	0.45
0.25	0.48
0.35	0.51
0.45	0.52
0.55	0.54
0.65	0.55
0.75	0.54
0.85	0.58
0.95	0.56

3. Kirkwood-Buff Analysis

The Kirkwood-Buff integrals are defined as[8]

$$G_{ij} = 4\pi \int_0^\infty r^2 \mathrm{d}r(g_{ij}(r) - 1) \tag{1}$$

where $g_{ij}(r)$ is the radial distribution function for species i and j. The physical interpretation of G_{ij} is best made in terms of the product $c_j G_{ij} = N_{ij}$ where c_j is the molar concentration of species j. N_{ij} can be interpreted as the excess number of particles of species j in the vicinity of a particle i.[18]

For electrolytes, special considerations are necessary in order to extract thermodynamic information from the KB integrals.[19] Since the concentrations of charged species are subject to the electroneutrality condition, they cannot be varied independently. This interdependency must be taken into account for KB theory to give meaningful results. For this reason, the expressions relating the KB integrals to thermodynamic properties are different for systems containing charged particles compared to those for systems with only neutral species. The concentration derivative of the chemical potential, μ, of a binary electrolyte is given by[19]

$$\frac{1}{k_B T}\left(\frac{\partial \mu}{\partial c}\right)_{T,p} = \frac{1}{c\Gamma} \tag{2}$$

with

$$\Gamma = c(G_{+-} - G_{+s}) = c(G_{+-} - G_{-s}) = \frac{N_{\mp\pm}}{\nu_\pm} - \frac{cN_{\mp s}}{c_s} \tag{3}$$

where c is the molar concentration and $\nu_\pm$ is the stoichiometric coefficient of the salt, i.e., $c_i = \nu_i c$ for the ions. The subscripts $+$, $-$, and s stand for cation, anion, and solvent, respectively. Below, we refer to Γ as "the binding parameter". (The definition of Γ is formally similar to that for the specific binding parameter in ternary solutions given as eq 9 in ref 20, but the thermodynamic significance is different.) Because of the electroneutrality condition for the KB integrals,[19] the expression for Γ is not unique; it can be rewritten in terms of G_{++} or G_{--} or in terms of a linear combination of G_{++}, G_{--}, and G_{+-}.

Γ in sodium sulfate was calculated using experimental mean activity coefficients and densities from ref 3. (The densities were required to make the conversion from molal to molar concentration scales.) The derivative in eq 2 was evaluated as a centered finite difference ratio. The results are summarized in Table 3.

As the Kirkwood−Buff theory is strictly valid only for systems that are open with respect to exchange of particles with their environments, there are some subtleties inherent in the evaluation of eq 1 from standard NpT MD simulations. Briefly, the main requirement for the calculation of the Kirkwood−Buff integrals with acceptable accuracy from simulation of a closed system is that the system size is large enough. This is met if the subsystem implicitly defined by the choice of cutoff for the integral in eq 2 approximates an open system, while the remainder of the simulation box plays the role of the environment.

In practice, we do not calculate Γ from $g_{ij}(r)$ but from the cumulative numbers $n_{ij}(r)$ of species j around species i according to[20]

$$\Gamma(r) = \frac{1}{\nu_\pm}\left(n_{\mp\pm}(r) - \frac{n_\pm - n_{\mp\pm}(r)}{n_s - n_{\mp s}(r)} n_{\mp s}(r)\right) \tag{4}$$

where n_i is the total number of particles of species i in the simulation box and $\Gamma(r)$ is the estimate of Γ for cutoff distance r. We approximate Γ by $\Gamma(r)$ for a sufficiently large value of r (14 Å). Comparison with test simulations for a larger system indicate that the error incurred by this procedure is less than ten percent. As the purpose of the comparison with experiments is not to find exact values of the optimal parameters for sulfate but rather to sort out models which are qualitatively unrealistic, this degree of accuracy is sufficient.

In systems where there is precipitation, Γ has no obvious thermodynamic meaning. The radial distribution functions obtained from simulation of such systems are not applicable to either the solid or solution bulk phase because the simulation contains the interfacial region between them, which is disproportionally important for small systems. Therefore, Γ could not be calculated for most of the systems where persistent clusters were formed. In run 3, precipitation did occur only after many nanoseconds and converged radial distribution functions unambiguously belonging to the solution phase could be obtained. Even though the association seen in run 8 (TIP4P/2005 water) may indicate either precipitation or association in the solution phase, see below, we have calculated Γ under the provisional assumption that the latter is the case.

4. Results

4.1. Ion Association in Sodium Sulfate Solutions. For sulfate models 1 and 2 together with sodium model 1 in SPC/E water (runs 1 and 2) extended clusters, comprising the majority of the ions in the simulation box, formed after several nanoseconds, see Figure 1. This behavior was observed also for the polarizable version of sulfate model 2 together with sodium model 1 in SPC/E water (run 9). For sulfate models 3 and 6 together with sodium model 1 (runs 3 and 6), clusters did not appear until after ∼15 ns, whereas for sulfate models 4 and 5 with the same sodium model (runs 4 and 5), clusters formed almost immediately. The clusters, once formed, were persistent, and ions in their interiors were stripped of their solvation shells. Thus, the clusters have the appearance of an incipient solid phase. The tentative conclu-

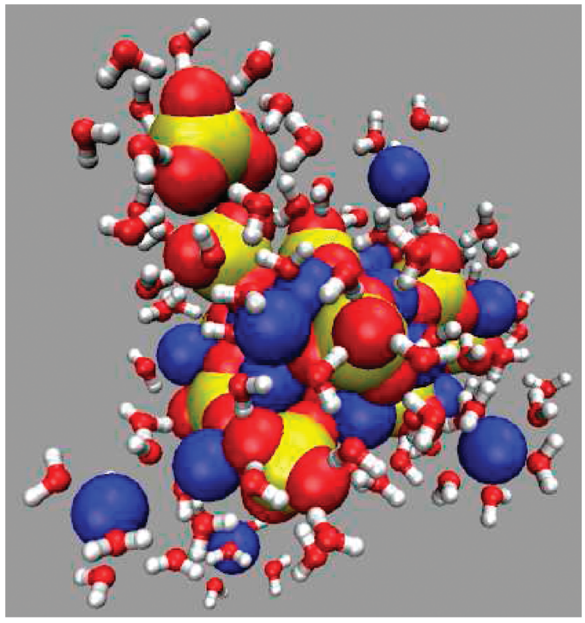

Figure 1. Snapshot from run 2 after 20 ns of simulation, showing the sodium and sulfate ions and all water molecules are within 3.0 Å of these.

sion is, therefore, that the cluster formation is due to precipitation, rather than association in the solution phase. We emphasize that further investigation is necessary to make a quantitative estimation of the solubility; the system size employed here is too small to draw quantitative conclusions about phase coexistence. Nevertheless, it is clear that almost complete association of the salt at 0.5 m concentration is not a realistic behavior for this electrolyte solution.

With the combination of sulfate model 2 and sodium model 2 (run 7), no persistent clusters were formed during the 30 ns simulation, although excessive ion pairing was still prevalent. For sulfate model 2 with sodium model 1 in TIP4P/2005 water (run 8), there was a large degree of association, but the clusters that formed in this system were not persistent. The ions participating in the aggregates in this system remained solvated, and there was exchange of ions between the cluster and the bulk throughout the simulation. In this case, it is, therefore, much more difficult to judge whether the clusters represent incipient precipitation or aggregates in the solution phase. In nature, sodium sulfate can crystallize either as a decahydrate (mirabilite) or as an anhydride (thenardite), which are close to each other in free energy at room temperature (see ref 21 for a phase diagram). The fact that ions remain hydrated in the clusters is, therefore, not necessarily evidence against incipient precipitation but may imply that in TIP4P/2005 water a hydrated solid phase is favored. The issue could in principle be resolved using a methodology similar to that in ref 22, but this is beyond the scope of the current study.

In contrast to the above simulations, none of the systems with polarizable water models, including that with nonpolarizable ions in POL3 water (runs 10, 11, and 12), displayed any cluster formation resembling precipitation. The radial distribution functions for these runs are shown in Figure 2. As can be seen in this figure, the two polarizable water models show remarkably similar structures with respect to ion pairing. Even though the first peak in the radial distribution function, corresponding to contact ion pairs, is the highest, the cumulative numbers show that solvent separated ion pairs, corresponding to the second peak, are more abundant. Nonpolarizable ions in POL3 water (run 9) have an enhanced tendency to form contact ion pairs between sodium and sulfate compared to polarizable ions, but the ionic polarizability has little effect on the overall structure beyond the first peak. The sulfate−sulfate radial distribution functions display a solvent-separated peak at around 6 Å for both water models, with depletion for other separations. The sodium−sodium radial distribution function displays a very

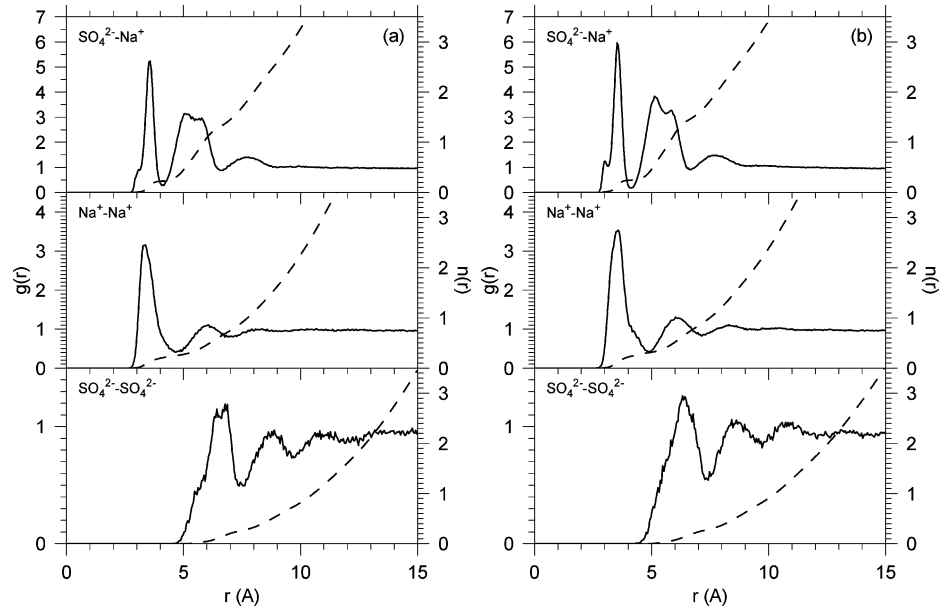

Figure 2. Radial distribution functions from runs 11 (subfigure a) and 12 (subfigure b), i.e., with POL3 and Dang−Chang water. The dashed lines are the cumulative numbers of ions (sodium ions for the SO_4^{2-}−Na^+ case).

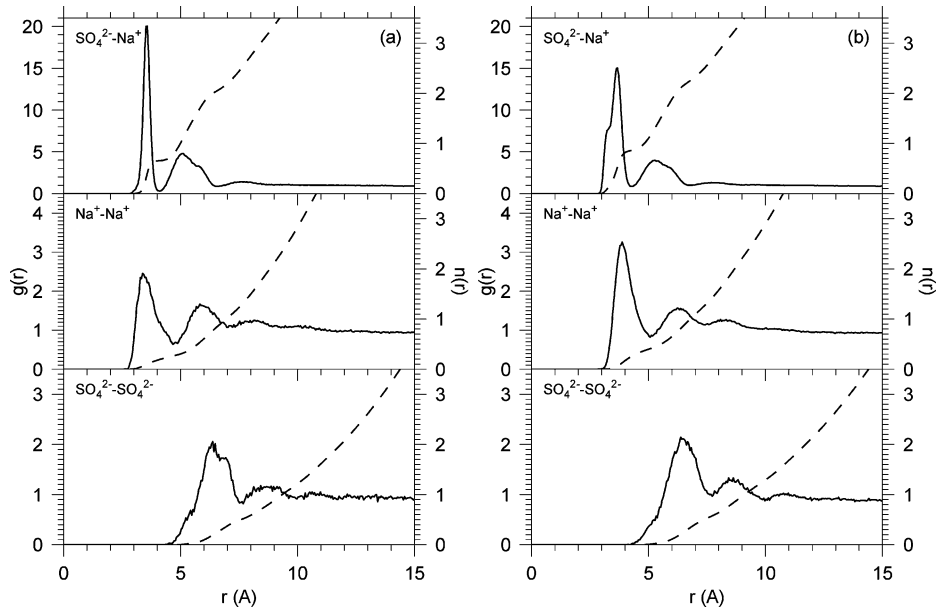

Figure 3. Radial distribution functions from the first 15 ns of run 3 (subfigure a) and run 7 (subfigure b), i.e., nonpolarizable runs with SPC/E water. The dashed lines are the cumulative numbers of ions (sodium ions for the SO_4^{2-}−Na^+ case).

pronounced peak at about 3 Å, which is due to simultaneous pairing of more than one sodium ion to a single sulfate ion.

The radial distribution functions for the two models with nonpolarizable water that remained unambiguously dissolved long enough for these to be calculated, i.e., sodium model 1 with sulfate model 3 (run 3) and sodium model 2 with sulfate model 2 (run 7), are shown in Figure 3. The sodium sulfate radial distribution functions for both of these models show a larger prevalence of both contact and solvent separated ion pairs than the models with polarizable water. Moreover, contact ion pairing is more strongly enhanced than solvent-separated pairing. The features of the sulfate−sulfate and sodium−sodium radial distribution functions are similar to those for the polarizable models, but for the nonpolarizable models, the values of the radial distribution functions are larger for all distances. This indicates a larger overall degree of association for the nonpolarizable models than for the polarizable ones. Although the overall structure is similar in the two nonpolarizable models, the shapes of the first peaks are somewhat different: for sulfate 3 with sodium 1, the peak is higher and narrower whereas for sulfate 2 with sodium 2 it is lower and has a pronounced shoulder toward smaller *r*.

The values of the binding parameter Γ for the different combinations of sodium, sulfate, and water parameters for which this quantity could be calculated are presented in Table 4. The experimental value of Γ for the concentration in the simulations of 0.48 m is 0.53. As can be seen from the table, all nonpolarizable models for which Γ could be evaluated, i.e., for which no persistent clusters formed, still predict values that are too large, by a factor two or more. The value for the TIP4P/2005 model of about 3 may reflect transient cluster formation and may, therefore, overestimate the association in the solution phase, as discussed above. Sulfate model 2 together with sodium model 1 in POL3 water agrees with the experimental value within the accuracy of the simulated values of Γ. Nonpolarizable ions in POL3 water and polarizable ions in Dang−Chang water give a bit higher value of Γ than the experiment and, thus, slightly overestimate the association in solution. The fact that Γ differs between POL3 and Dang−Chang water despite the observation that the radial distribution functions are similar, Figure 2, indicates that Γ is a very sensitive measure of the degree of association in the electrolyte.

Table 4. Binding Parameter Γ Calculated According to Eq 4

water	sulfate model	sodium model	Γ
SPC/E	3	1	1.1
SPC/E	2	2	1.1
TIP4P/2005	2	1	3
POL3	2	1	0.54
POL3	2[a]	1[a]	0.71
Dang-Chang	2	1	0.72
experiment			0.53

[a] Nonpolarizable ions.

4.2. Polarization of the Solvation Shell. The first solvation shell of sulfate in the simulations typically contained 11 to 12 water molecules, most commonly with three water molecules hydrogen bonding to each sulfate oxygen in a tetrahedral arrangement. A typical snapshot from the simulation of the solvent shell around a single sulfate ion in POL3 water is shown in Figure 4. The solvation structure did not depend significantly on the choice of water model.

To quantify the polarization in the vicinity of a sulfate ion, we calculated the average magnitude of the induced dipole moment of water molecules as a function of distance from the ion. In Figure 5, results are shown for sulfate model 2 in POL3 and Dang−Chang waters. In POL3 water, the average induced dipole moment in the water bulk is around 0.59 D, while in the first solvation shell of sulfate it reaches a value of 0.70 D. For the Dang−Chang water model, the average induced dipole moment in bulk is 0.88 D, reaching 0.99 D in the first solvation shell. The distance dependence of the deviation in induced dipole moment from the bulk value is almost identical for the two water models. The

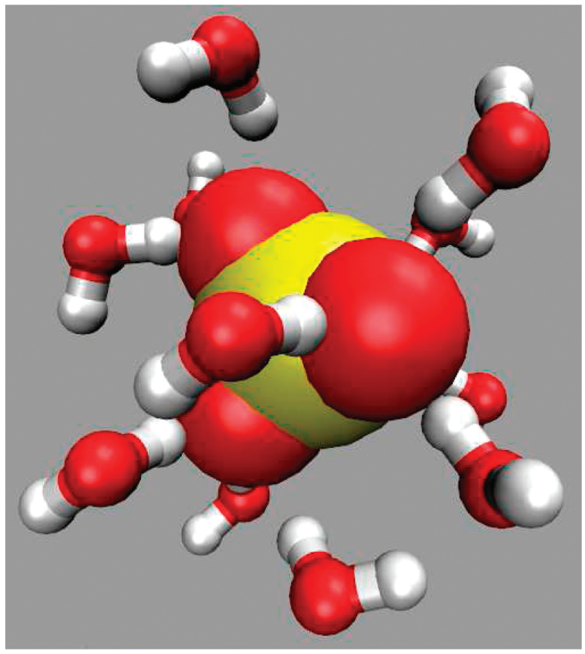

Figure 4. Snapshot from the simulation of one sulfate ion in water, showing the sulfate ion and all water molecules within 3.0 Å.

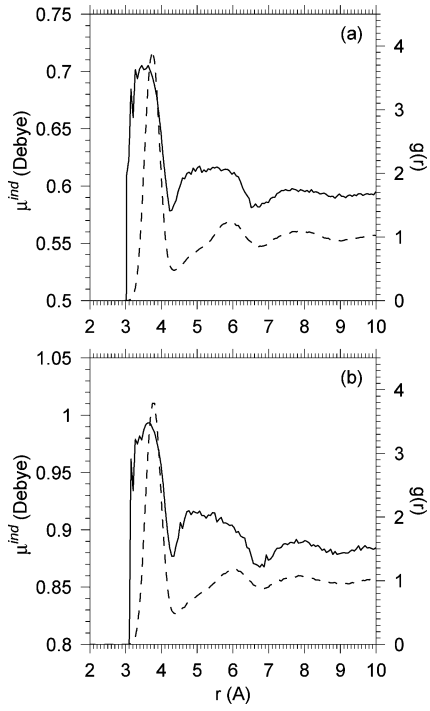

Figure 5. Average induced dipole moment of water molecules as a function of the center of mass distance from an ion (full curve). The ion−water center of mass radial distribution function is also shown (dashed curve) for reference. Panel (a) is for POL3 water and panel (b) is for Dang−Chang water.

structure of the induced dipole moment profile follows that of the radial distribution function with both the first and second solvation shells discernible. It is remarkable that the two water models agree to such an extent about the change in induced dipole moment caused by the presence of a sulfate ion, event though the bulk values differ by one-third.

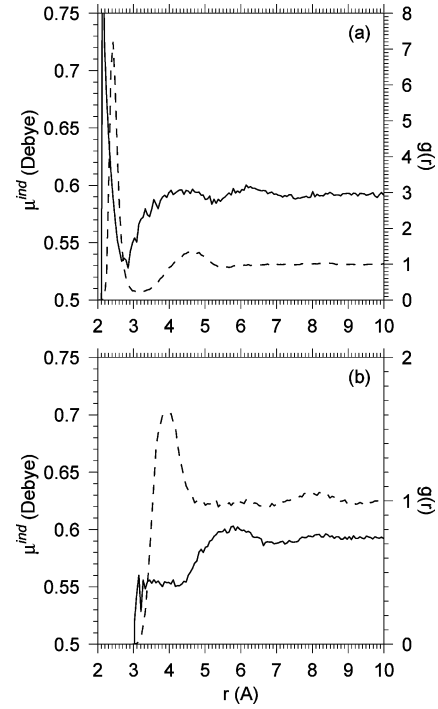

Figure 6. Same as Figure 5, but for sodium (panel a) and an ion model that is identical to sulfate model 2 except that all partial charges are halved (panel b).

For sodium, the polarization profile has a region close to the ion where the induced dipole moment is smaller than in bulk, but for very small sodium−water distances, the induced dipole moment becomes larger than in the bulk, Figure 6a. The polarization profile crosses the bulk value almost exactly at the position of the first maximum of the radial distribution function. The water molecules participating in the first solvation shell have, therefore, on average over the whole shell, an induced dipole moment similar to that of water molecules in bulk.

To separate the effect of ionic valency from geometric issues, we also carried out similar calculations for a monovalent version of sulfate model 2, where all partial charges are halved (Figure 6b). Thus, the electric field originating from the ion is halved, save for the contribution due to induced dipoles. For this model ion, the first peak in the induced dipole profile is absent. In fact, the first solvation shell is less polarized than bulk water.

5. Discussion

In the nonpolarizable simulations of sodium sulfate solutions, the values of the binding parameter Γ are significantly lager than in any of the polarizable ones. This indicates that polarizability strongly influences interactions in the solution phase as well as the apparent solubility. Since the binding parameter Γ is an integral quantity, the comparison of experimental and simulated values cannot constitute a definitive test of the quality of the description of the structural details of the electrolyte. The adequacy of a model with respect to finer structural details, in particular the relative abundances of contact and solvent-separated ion pairs, must be tested by other means. Raman spectroscopy does not give indication of a strong presence of contact ion pairs in aqueous

sodium sulfate solutions.[23] Similarly, dielectric relaxation spectra can be rationalized using the assumption that solvent separated and doubly solvent separated ion pairs are dominant over contact ion pairs.[24] Thus, also in structural aspects, the polarizable models, which predict predominance of solvent-separated ion pairs, are more realistic than the nonpolarizable ones, which yield extensive contact ion pairing and clustering.

Excessive association is found for all variations of the sulfate model examined in SPC/E water. An increase in the sodium ion σ can inhibit cluster formation on the time scale of the present simulations; however, the experimental binding parameter cannot be reached within realistic sizes for Na^+. Moreover, the excessive association is not limited to sodium cations. Indeed, we have observed that polycationic peptides associate strongly with sulfate model 2 in SPC/E water, with association being reduced in POL3 water in the same way as for sodium sulfate.[25]

From the differences between the simulations with polarizable and nonpolarizable water models and the similarity between the two polarizable models, it follows that partial suppression of contact ion pairing is primarily an effect of polarizability. A similar, albeit weaker, effect of polarizability was previously observed in suppressed contact ion pairing between cationic amino acid side chains and halide ions.[26] This behavior begs the explanation of the mechanism by which polarizability influences ion pairing.

If polarization of the first solvation shell of an ion is larger than the average polarization of bulk water, the polarization energy will give a stabilizing contribution to the free energy of solvation. It has been noted that inclusion of polarizability tends to make the free energy of solvation of both neutral and charged species more negative.[27] For charged solutes in water, however, this contribution accounts only for a small fraction of the total solvation free energy.

The free energy change associated with the replacement of a hydration water with a cation is sensitive to the marginal change in solvation energy due to solvent polarization since it is a result of a subtle balance between ion−ion and ion−water interactions. Replacement of a polarizable water molecule with a practically nonpolarizable sodium ion carries with itself a larger free energy cost than the corresponding replacement of a nonpolarizable water molecule. The free energy cost need not be large compared to the solvation free energy to have a significant effect on the overall behavior of the system; the difference between the radial distribution functions in Figures 2 and 3 corresponds to a difference in the minimum of the potential of mean force of about 1 k_BT. As the hydration shell of sulfate is more polarized than the bulk water and therefore stabilized, the suppression of contact ion pairing in polarizable water models is consistent with this rationalization. Note that in other cases, where the solvation shell would be destabilized by polarization, contact ion pairing could be enhanced in polarizable water. In fact, the inclusion of polarizability in the force field has been found to cause an increase in contact ion pairing in model strontium chloride.[28] This illustrates that the effect of polarizability on interionic interactions is dependent on the details of the system.

It has recently been noted that certain combinations of commonly used models for the alkali metal cations and the halides display pathological behavior such as an unrealistically low solubility and excessive ion pairing, similar to what we have observed here.[22,29–32] For the alkali halides, systematic parametrizations compatible with nonpolarizable water models have recently been successfully developed.[22,33–35] Thus, in contrast to sulfate salt solutions, polarizability does not seem to play an essential role for the description of ion pairing in simple monovalent salt solutions. This difference can be reconciled by the fact that the strength of the field acting on, and thereby polarizing, the water molecules in the first solvation shell of divalent ions is stronger than that of monovalent ions.

6. Conclusions

We investigated different variants of nonpolarizable potential models of the sulfate dianion,[1] together with polarizable versions of that model[6] and different models of water and the sodium cation. Nonpolarizable models consistently and significantly overestimate the degree of association in the system. For most of these models, there is precipitation of the salt already at relatively low concentrations and even when the salt is soluble there is excessive ion pairing. In contrast, for polarizable models, only a modest degree of association is observed, which is consistent with the activity coefficients of real sodium sulfate solutions. This effect is mainly due to polarization of water molecules; simulations with nonpolarizable ions in a polarizable water are more similar to the fully polarizable simulations than simulations with polarizable ions in a nonpolarizable water. While the degree of association is to some extent sensitive to the choice of Lennard−Jones parameters, we did not find a combination of parameters that would give a physically reasonable association behavior using a nonpolarizable water model. These results indicate that simulations of sulfate-containing systems using nonpolarizable water are liable to produce artifacts in the form of severely overestimated association.

Acknowledgment. Support from the Czech Ministry of Education (Grant LC 512), the Czech Science Foundation (Grant 203/08/0114), and the Academy of Sciences (Praemium Academie) is gratefully acknowledged.

References

(1) Cannon, W. R.; Pettitt, B. M.; McCammon, J. A. *J. Phys. Chem.* **1994**, *98*, 6225–6230.

(2) Smith, D. E.; Dang, L. X. *J. Chem. Phys.* **1994**, *100*, 3757–3766.

(3) Lide, D. R., Ed. *Handbook of Chemistry and Physics (Internet Version)*, 90th ed.; CRC Press: Boca Raton, FL, 2010; Section 8, pp 112−117; Section 8, pp 52−77; Section 5, pp 79−80.

(4) Cerutti, D. S.; Le Trong, I.; Stenkamp, R. E.; Lybrand, T. P. *Biochemistry* **2008**, *47*, 12065–12077.

(5) Huige, C. J. M.; Altona, C. *J. Comput. Chem.* **1995**, *16*, 56–79.

(6) Jungwirth, P.; Curtis, J. E.; Tobias, D. J. *Chem. Phys. Lett.* **2003**, *367*, 704–710.

(7) Gopalakrishnan, S.; Jungwirth, P.; Tobias, D. J.; Allen, H. C. *J. Phys. Chem. B* **2005**, *109*, 8861–8872.

(8) Kirkwood, J. G.; Buff, F. P. *J. Chem. Phys.* **1951**, *19*, 774–777.

(9) Essmann, U.; Perera, L.; Berkowitz, M. L.; Darden, T.; Lee, H.; Pedersen, L. G. *J. Chem. Phys.* **1995**, *103*, 8577–8593.

(10) Berendsen, H. J. C.; Postma, J. P. M.; van Gunsteren, W. F.; DiNola, A.; Haak, J. R. *J. Chem. Phys.* **1984**, *81*, 3684–3690.

(11) Case, D. A.; Darden, T. A.; Cheatham, T. E., III; Simmerling, C. L.; Wang, J.; Duke, R. E.; Luo, R.; Crowley, M.; Walker, R. C.; Zhang, W.; Merz, K. M.; Wang, B.; Hayik, S.; Roitberg, A.; Seabra, G.; Kolossváry, I.; Wong, K. F.; Paesani, F.; Vanicek, J.; Wu, X.; Brozell, S. R.; Steinbrecker, T.; Gohlke, H.; Yang, L.; Tan, C.; Morgan, J.; Hornak, V.; Cui, G.; Mathews, D. H.; Seetin, M. G.; Sagui, C.; Babin, V.; Kollman, P. A. *AMBER 10*; University of California: San Fransisco, 2008.

(12) Roselova, M.; Jungwirth, P.; Tobias, D. J.; Gerber, R. B. *J. Phys. Chem. B* **2003**, *107*, 12690–12699.

(13) Thole, B. T. *Chem. Phys.* **1981**, *59*, 341–350.

(14) Caldwell, J. W.; Kollman, P. A. *J. Phys. Chem.* **1995**, *99*, 6208–6219.

(15) Dang, L. X.; Chang, T.-M. *J. Chem. Phys.* **1997**, *106*, 8149–8159.

(16) Berendsen, H. J. C.; Grigera, J. R.; Straasma, T. P. *J. Phys. Chem.* **1987**, *91*, 6269–6271.

(17) Abascal, J. L. F.; Vega, C. *J. Chem. Phys.* **2005**, *123*, 234505.

(18) Hall, D. G. *Trans. Faraday Soc.* **1971**, *67*, 2516–2524.

(19) Kusalik, P. G.; Patey, G. N. *J. Chem. Phys.* **1987**, *86*, 5110–5116.

(20) Pierce, V.; Kang, M.; Aburi, M.; Weerasinghe, S.; Smith, P. E. *Cell Biochem. Biophys.* **2008**, *50*, 1–22.

(21) Flatt, R. J. *J. Cryst. Growth* **2002**, *242*, 435–454.

(22) Joung, I. S.; Cheatham, T. E., III. *J. Phys. Chem. B* **2009**, *113*, 13279–13290.

(23) Daly, F. P.; Brown, C. W.; Kester, D. R. *J. Phys. Chem.* **1972**, *76*, 3664–3667.

(24) Buchner, R.; Capewell, S. G.; Hefter, G.; May, P. M. *J. Phys. Chem. B* **1999**, *103*, 1185–1192.

(25) Wernersson, E.; Heyda, J.; Kubíčková, A.; Křížek, T.; Coufal, P.; Jungwirth, P. *J. Phys. Chem. B* **2010**, *114*, 11934–11941.

(26) Heyda, J.; Hrobárik, T.; Jungwirth, P. *J. Phys. Chem. A* **2009**, *113*, 1969–1975.

(27) Geerke, D. P.; van Gunsteren, W. F. *J. Phys. Chem. B* **2007**, *111*, 6425–6436.

(28) Smith, D. E.; Dang, L. X. *Chem. Phys. Lett.* **1994**, *230*, 209–214.

(29) Auffinger, P.; Cheatham, T. E., III; Vaiana, A. C. *J. Chem. Theory Comput.* **2007**, *3*, 1851–1859.

(30) Chen, A. A.; Pappu, R. V. *J. Phys. Chem. B* **2007**, *111*, 11884–11887.

(31) Fennell, C. J.; Bizjak, A.; Vlachy, V.; Dill, K. A. *J. Phys. Chem. B* **2009**, *113*, 6782–6791.

(32) Fennell, C. J.; Bizjak, A.; Vlachy, V.; Dill, K. A.; Sarupria, S.; Rajamani, S.; Garde, S. *J. Phys. Chem. B* **2009**, *113*, 14837–14838.

(33) Horinek, D.; Mamatkulov, S. I.; Netz, R. R. *J. Chem. Phys.* **2009**, *130*, 124507.

(34) Joung, I. S.; Cheatham, T. E., III. *J. Phys. Chem. B* **2008**, *112*, 9020–9041.

(35) Fyta, M.; Kalcher, I.; Dzubiella, J.; Vrbka, L.; Netz, R. R. *J. Chem. Phys.* **2010**, *132*, 024911.

CT100465G